EVALUATION OF WITHDRAWAL STRENGTH OF SELF-TAPPING SCREWS INSERTED INTO CROSS-LAMINATED TIMBER WITH DIFFERENT ANATOMICAL ASPECTS

Sarah Amira
Doctoral Student
Department of Bioresource Sciences
United Graduate School of Agricultural Science
Gifu University (placement at Shizuoka University)
836 Ohya, Suruga Ward, Shizuoka 422-8529, Japan
E-mail: sarah.amira.19@shizuoka.ac.jp

*Kenji Kobayashi**
Associate Professor
Department of Bioresource Sciences
Faculty of Agriculture
Shizuoka University
836 Ohya, Suruga Ward, Shizuoka 422-8529, Japan
E-mail: kobayashi.kenji.b@shizuoka.ac.jp

Keita Ogawa
Assistant Professor
Department of Bioresource Sciences
Faculty of Agriculture
Shizuoka University
836 Ohya, Suruga Ward, Shizuoka 422-8529, Japan
E-mail: ogawa.keita@shizuoka.ac.jp

(Received September 2023)

Abstract. The use of cross-laminated timber (CLT) technology is witnessing an upsurge in Japan because of its satisfactory performance under seismic conditions. The withdrawal strength (f_{ax}) of a single self-tapping screw (STS) inserted into the CLT was investigated using a withdrawal test. The experimental results showed that f_{ax} of the partially threaded STS was higher than that of the fully threaded STS when inserted perpendicular to the grain. The empirical model used to predict f_{ax} provided in the European standard for the design of timber structures was evaluated by comparing the predicted values with the experimental results, which showed that the empirical model was only suitable for predicting the withdrawal strength of specimens with STSs inserted perpendicular to the grain. Therefore, a new probabilistic model was proposed for specimens inserted with STSs inserted parallel to the grain. The failure modes with respect to the orthotropic anatomy of wood materials were investigated.

Keywords: Withdrawal strength, probabilistic model, failure mode.

INTRODUCTION

Timber construction techniques have been used to construct temples and shrines in Japan since ancient times. Most residential houses in Japan are also constructed using wood. Cross-laminated timber (CLT) is an engineered wood product used in wooden houses to achieve environmental sustainability in Europe, Australia, and North America. Interest in CLT as a newly developed technology has increased in Japan. Izzi et al (2018) stated that CLT structures exhibited satisfactory performance under seismic conditions because of the high strength-to-weight ratio and in-plane stiffness of the CLT panels and the capacity of connections to resist loads with ductile deformations and limited strength impairment.

* Corresponding author

Self-tapping screws (STSs) optimized mainly for axial loading represent a state-of-the-art fastening and reinforcement technology in CLT construction. STSs are highly recommended by CLT manufacturers and designers, both overseas and in Japan, owing to their economic benefits and easy handling (Mohammad et al 2013; Kobayashi 2015; Dietsch and Brandner 2015). Recently, the Japanese Industrial Standard for STSs for timber joints (JIS A 1503) has been published. However, this standard does not include withdrawal strength and head pull-through properties because their inclusion requires the consideration of the properties of the adjacent wood; the JIS is primarily focused on the fastener property (Goto et al 2018). CLT buildings in Japan are primarily constructed for residential use and restricted to three stories because of the limited local wood sources, which results in costly and unaffordable CLT production (Passarelli and Koshihara 2018). The lack of standards for CLT structures in Japan renders it difficult to assess the mechanical strength of wood panels and the capacity of connectors to resist loads. An analytical approach for CLT connections is necessary to precisely design CLT constructions and allow for the efficient use of wood in the future.

The raw material for CLT structures should be sourced from species that are readily available in sufficient quantities. Indonesia, in Southeast Asia, has a topography similar to that of Japan and faces the common problem of being an earthquake-prone area. Southeast Asia has one of the oldest tropical forests in the world and supplies large volumes of wood-based products to the world (Okuda et al 2018). The growth of trees as the source of raw wood materials from tropical natural forests, particularly trees of large diameter with high-quality wood, requires long rotations and this resource has been the target of reckless exploitation. In response to this challenge, Indonesia has planted fast-growing tree species to reduce the use of natural forest trees. Some plantation species in the tropics may grow faster than those in temperate climates because of year-round favorable environmental conditions. Fast-growing plantation species, such as jabon (*Neolamarckia cadamba* (Roxb.) Bosser), show a relatively high mean annual increment, with a growth of 7-10 cm/yr in diameter and 3-6 m/yr in height within 5 yr (Mansur and Tuheteru 2010).

Neolamarckia cadamba, commonly known in English as burflower-tree and locally known as kadam or jabon, demonstrates high prospects for industrial plantations and reforestation in Indonesia. This species is also expected to become increasingly important for the timber industry in the future, particularly when wood-based raw materials from natural forests are expected to decrease in the coming years (Krisnawati et al 2011). The wood from this species is typically easy to work with hand tools and machines. It can be easily sawn, crosscut, and planed, and the resulting planed surface is smooth. However, its use is mostly limited to furniture, plywood, pulp, and chips, and it is not yet as major structural timber components in the construction sector (Okuda et al 2018). Moreover, CLT reference standards are not available for jabon wood properties and their connection performance. The use of this species for CLT construction requires that its properties be investigated against those of several common commercial species used for CLT.

Parameters that mainly influence fastener behavior include the axial strength of the fastener, the density of the wood in which it is inserted, and the direction of loading with respect to the grain orientation (Mahdavifar et al 2018). Previously, studies were conducted on the withdrawal capacity of an STS in a single-layered timber and CLT using a probabilistic approach covering the entire density and diameter bandwidths (Ringhofer et al 2015; Brandner et al 2018; Brandner 2019). However, the length of the inserted STS-threaded part was not considered to be included in the proposed model.

The present study investigates the withdrawal performance of STSs inserted into CLT with respect to the density of the timber species, the effective insertion length of the STS-threaded part, and the CLT side with the STS insertion. The experimental results were compared with the design equation in current regulation EN 1995-1-1:2004/A1

(2008) and commonly recited probabilistic approaches. The scope of withdrawal strength parameters in this study necessitated a specific probabilistic model approach. Moreover, the types of failures that occurred in the withdrawal test were also investigated.

MATERIALS AND METHODS

Materials

The withdrawal strength of a single STS inserted into CLT was measured using a withdrawal-loaded test. The specimens used in this study were composed of small pieces of CLT and glue-laminated timber (GLT) with two types of STSs (fully threaded and partially threaded). Jabon (*Neolamarckia cadamba* (Roxb.), sourced from Medan, Indonesia, was used as a representative fast-growing Indonesian hardwood. Sugi (*Cryptomeria japonica* D. Don), hinoki (*Chamaecyparis obtusa*), and karamatsu (*Larix kaempferi*) wood species were used as the representative commercial Japanese softwood species.

Lamina selection is a prerequisite of the CLT manufacturing process that minimizes defects and substandard quality in the final product. Once the lamina materials were visually selected to exclude knots, decay, and finger joints (on jabon materials), they were classified physically and mechanically. The laminas were conditioned at a constant temperature of 20 ± 2 and 65% RH for 2 wk, assuming the MC reached an EMC. The mean density ρ (kg/m^3) for entire laminas at air-dried conditions was calculated using the gravimetry method, as depicted in Eq 1.

$$\rho = \frac{m}{V}, \tag{1}$$

where m is the lamina mass (kg) and V is the lamina volume (m^3). The lamina materials were graded according to the Japanese Agricultural Standard for CLT (JAS 3079-2013) by determining the value of their Young's moduli in bending. The large-sized jabon wood as a raw material from Indonesia was not easily imported. For this reason, the limited size of jabon wood was obtained from furniture producer Ōta Sangyō Co., Ltd., and a distinctive technique to measure its basic properties was required. The jabon laminas were sawn, trimmed, and planned to produce 3900-mm length, 40-mm wide, and 25-mm thick specimens with two flatwise finger joints. The laminas were used to prepare clear specimens that were at least 200-mm long. Furthermore, the total length (L) was subcategorized into 200 mm $\leq L <$ 330 mm and $L \geq$ 330 mm. Static bending tests were conducted according to JIS Z 2101 (2009) to the 132 laminas with $L \geq$ 330 mm, and the bending span between the fulcrums was 300 mm. Young's modulus in bending E_b (GPa) was calculated using the following expressions:

$$E_b = \frac{l^3 \Delta P}{48 I \Delta y}, \tag{2}$$

$$I = \frac{bh^3}{12}, \tag{3}$$

where l is the bending span (mm); I is the moment inertia of area (mm^4); ΔP is the change in load in the proportional limit area (kN); Δy is the deflection at the center of the span corresponding to ΔP (mm); b is the width of the cross section (mm); and h is the thickness (mm); and $\Delta P/\Delta y$ is the slope of load and deflection changes in the elastic range. The obtained mean Young's modulus in bending of jabon lamina was 6.812 GPa with a 0.205 coefficient of variation. Eleven of 132 laminas were classified into M 30A grade ($E_b \geq$ 2.5 GPa), the rest were classified into M 60A grade ($E_b \geq$ 5 GPa).

Compression tests were carried out on the shorter 304 laminas according to JIS Z 2101 (2009). The measurement of Young's modulus in compression was aimed at approaching Young's modulus in bending value. Thirty-two laminas with the $L \geq$ 330 mm also were compression tested. The linearity between Young's modulus in bending value and Young's modulus in compression was analyzed to correct Young's modulus in compression. The longitudinal Young's modulus in compression E_c (GPa) was calculated using the following formula:

$$E_c = \frac{\Delta P l}{\Delta l A}, \tag{4}$$

where A is the cross-sectional area of specimen (mm^2); ΔP is the difference between the upper limit load and the lower limit load in the proportional limit area (kN); l is the clamping span (mm) which was set at 160 mm; and Δl is shrinkage corresponding to ΔP (mm). After Young's modulus in compression for the shorter laminas with 200 mm $\leq L <$ 330 mm were corrected into Young's modulus in bending, the obtained mean Young's modulus in the bending of jabon lamina was 6.614 GPa with a coefficient of variation of 0.369. Seventeen laminas were underrated and eliminated, 93 laminas were classified into M 30A grade, and 194 laminas were classified into M 60A grade according to JAS 3079-2013.

Lamina selection of the Japanese species was solely to eliminate defects and knots along the lamina after the bending test had been conducted. Sugi laminas were classified into the M 60A to M 120A ($E_b \geq 10$ GPa) grades, whereas hinoki and karamatsu laminas were classified into the M 90A ($E_b \geq 7.5$ GPa) to M 120A grades. Lamina grading was used as a reference for CLT assembly configuration. Laminas with lower grades were configured for the inner layers, and the higher-graded laminas were configured for the outer layers in this study.

The test specimens were manufactured as five-layer CLT. In addition, GLT specimens were manufactured to approximate the assumed closest values to solid wood. The laminas were adhered using the aqueous polymer isocyanate (API) adhesive TP-111 at a ratio of 100:15 to a cross-linking agent. The glue spread rate was 250 g/m^2, with a double glue line for face and edge bonding. Using a compressive machine, the assemblies were adjusted with pressures of 1 MPa and retained under pressure at 20°C for 30 min. The API-bonded specimens were produced and conditioned at 65 ± 5% RH and 20 ± 2°C for 2 wk to reach EMC close to 12%.

Three positions in the CLT were available for the STS insertion: A, the plane side of the CLT; B, narrow side parallel to the grain of the CLT core layer; and C, narrow side perpendicular to the grain of the CLT core layer. Type A was composed of five layers, whereas types B and C were composed of three layers as the expected effective layers. Ten replicates were used for each combination series. The design of specimen dimensions and STS insertion points is shown in Fig 1. The insertion point of the STS on the CLT was determined according to the European standards for the design of timber structures (EN 1995-1-1

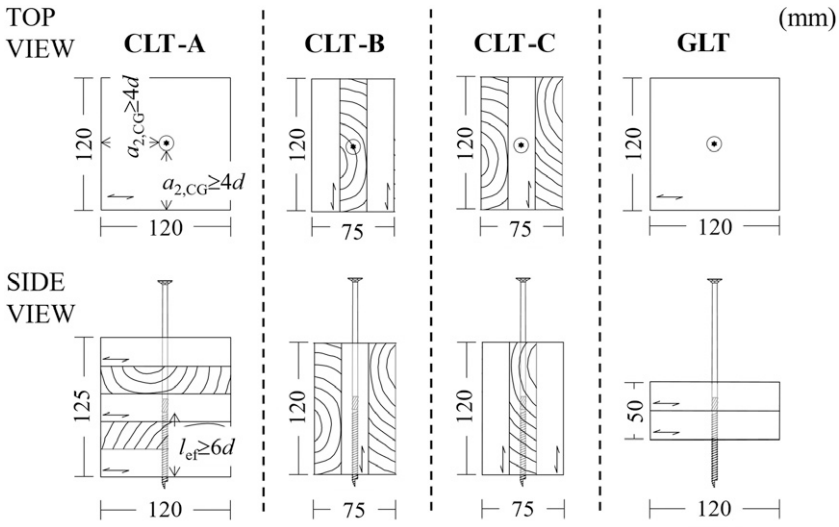

Figure 1. The design of specimen dimensions and the STS insertion point.

2004 and EN 1995-1-1:2004/A1 2008) by applying the minimum edge distance of the center of gravity of the threaded part of the STS in each layer. Fully threaded STS (PX8-260) and partially threaded STS (PS8-260) connectors, manufactured by Synegic Co., Ltd., with a thread diameter of 8 mm and the total length L of 260 mm, as illustrated in Fig 2, were considered and distinguished by the effective length of the STS-threaded part inserted into the specimen. The shapes of the screw head, compressor, and screw tip were assumed not to contribute to the measurements. The l_{ef} of specimens with partially threaded STSs was set into 32 mm for GLT and 80 mm for CLT, while those of fully threaded STSs depended on the dimension of the specimen that is in line with the withdrawal test direction. The nomenclature of the specimens included the first letter of the wood species (S for sugi, J for jabon, H for hinoki, and K for karamatsu), followed by the first letter of the STS type (P for partially threaded STS and F for fully threaded STS), and the last character indicating the type of specimen and its STS insertion point (GLT, CLT-A, CLT-B, and CLT-C). Table 1 lists the mean values of the lamina material density (ρ) and the effective length of the fully threaded STS (l_{ef}) measured from the bottom face of the CLT for each series.

Withdrawal Test

The STS was driven through the entire test specimen to avoid the tip influencing the layer orientation, as shown in Fig 1. A turned washer with a diameter of 8 mm was used to fix the screw head to the screw grip. The withdrawal test apparatus is illustrated in Fig 3. A screw grip shaped to fit the head of the STS was attached to the load head of a universal testing machine Shimadzu Co., AG-I 250 kN. Two displacement gauges (CDP-25) with a capacity of 25 mm (manufactured by the Tokyo Instruments Laboratory Co., Ltd.) were attached to the steel plate and the pitches of the displacement gauges were adjusted to the right and the left side 100 mm from the center of the STS against the plastic plate which was attached to the STS body above the CLT to record the displacement between the STS and the steel plate above the CLT during the withdrawal test.

Monotonic static loading was performed at a constant rate of 1 mm/min. The maximum load, F_{max} was determined, and the f_{ax} (N/mm^2) was calculated using the following equation (Ringhofer et al 2015; Brandner 2019) according to EN 1382 (1999) with π included in the divisor:

$$f_{ax} = \frac{F_{max}}{d\pi l_{ef}}, \tag{5}$$

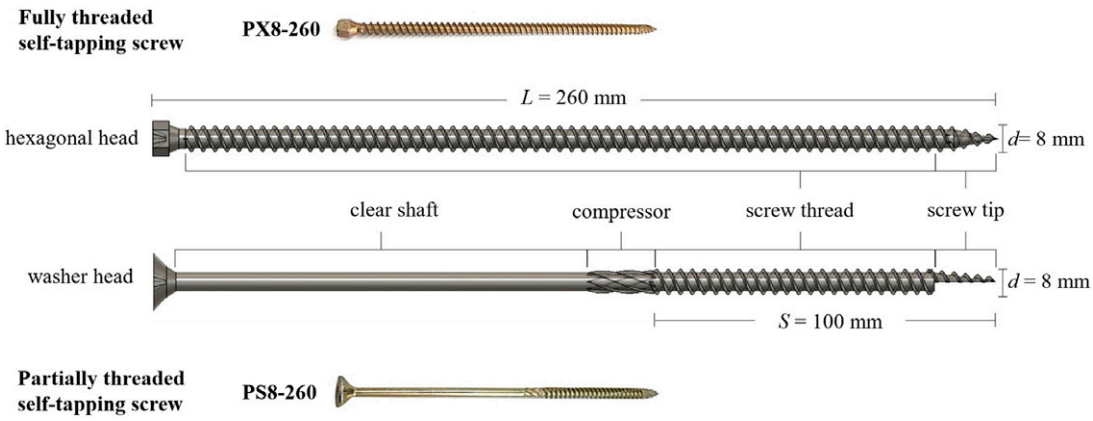

Figure 2. Connector properties showing the fully threaded self-tapping screw (above) and partially threaded self-tapping screw (below).

Table 1. Mean values of lamina density (ρ) and effective insertion length of STS-threaded parts (l_{ef}) for each series.

					ρ		l_{ef}	
Series	Species	Screw type	Specimen type	*n* #	Mean (kg/m^3)	CoV (%)	Mean (mm)	CoV (%)
S.P.GLT	Sugi	Partially threaded	GLT	10	366.7	5.8	32	—
S.P.CLT-A			CLT-A	10	349.2	2.9	80	—
S.P.CLT-B			CLT-B	10	373.0	2.8	80	—
S.P.CLT-C			CLT-C	10	367.3	2.5	80	—
S.F.GLT		Fully threaded	GLT	10	369.9	4.8	50.9	0.2
S.F.CLT-A			CLT-A	10	376.9	5.7	127.1	0.2
S.F.CLT-B			CLT-B	10	372.4	2.8	120.4	0.7
S.F.CLT-C			CLT-C	10	363.0	5.3	120.3	1.1
J.P.GLT	Jabon	Partially threaded	GLT	10	402.7	2.3	32	—
J.P.CLT-A			CLT-A	10	448.3	3.6	80	—
J.P.CLT-B			CLT-B	10	411.5	4.2	80	—
J.P.CLT-C			CLT-C	10	410.4	3.5	80	—
J.F.GLT		Fully threaded	GLT	10	425.3	7.5	49.5	0.1
J.F.CLT-A			CLT-A	10	426.7	2.9	123.7	0.1
J.F.CLT-B			CLT-B	10	414.2	4.8	118.3	1.4
J.F.CLT-C			CLT-C	10	411.1	3.9	121.5	0.4
H.P.GLT	Hinoki	Partially threaded	GLT	10	409.2	2.0	32	—
H.P.CLT-A			CLT-A	10	432.6	3.8	80	—
H.P.CLT-B			CLT-B	10	439.2	4.0	80	—
H.P.CLT-C			CLT-C	10	473.9	5.1	80	—
H.F.GLT		Fully threaded	GLT	10	409.6	2.0	50.8	0.2
H.F.CLT-A			CLT-A	10	432.8	2.2	126.7	1.7
H.F.CLT-B			CLT-B	10	455.7	2.1	120.3	0.4
H.F.CLT-C			CLT-C	10	448.7	2.2	118.9	0.5
K.P.GLT	Karamatsu	Partially threaded	GLT	10	515.3	5.2	32	—
K.P.CLT-A			CLT-A	10	524.4	1.4	80	—
K.P.CLT-B			CLT-B	10	524.5	2.5	80	—
K.P.CLT-C			CLT-C	10	525.9	2.2	80	—
K.F.GLT		Fully threaded	GLT	10	548.3	4.0	50.5	5.2
K.F.CLT-A			CLT-A	10	530.6	4.4	126.0	2.5
K.F.CLT-B			CLT-B	10	541.7	2.8	120.8	0.3
K.F.CLT-C			CLT-C	10	539.2	1.2	120.4	0.3

where F_{max} is the maximum load attained in each test (N); d is the thread diameter (mm); and l_{ef} is the effective insertion length of the threaded part (mm).

According to EN 1995-1-1:2004/A1 (2008), the characteristic withdrawal parameter of a single screw f_p (N/mm^2) is calculated as follows:

$$f_p = 0.52 d^{-0.5} l_{ef}^{-0.1} \rho_k^{0.8}, \quad (6)$$

where d is the thread diameter (mm), l_{ef} is the effective insertion length of the threaded part of the STS (mm), and ρ_k is the characteristic density adjusted the 12% MC value (kg/m^3). This equation should be divided by π such that the result can be compared with the experimental value of withdrawal strength obtained from Eq 5. Thus, a comparative equation was generated as follows:

$$f_{ax,EC5} = \frac{= 0.52 d^{-0.5} l_{ef}^{-0.1} \rho_k^{0.8}}{\pi}, \quad (7)$$

Furthermore, the lower 5%-quantile value, assuming a normal distribution of the experimental results, was calculated using the following equation (AIJ 2006).

$$5\% - \text{quantile value} = \overline{x}\ (1 - k\ CV), \quad (8)$$

where $\overline{x}$ is the mean value, k is the coefficient for obtaining the 95% lower tolerance limit at the

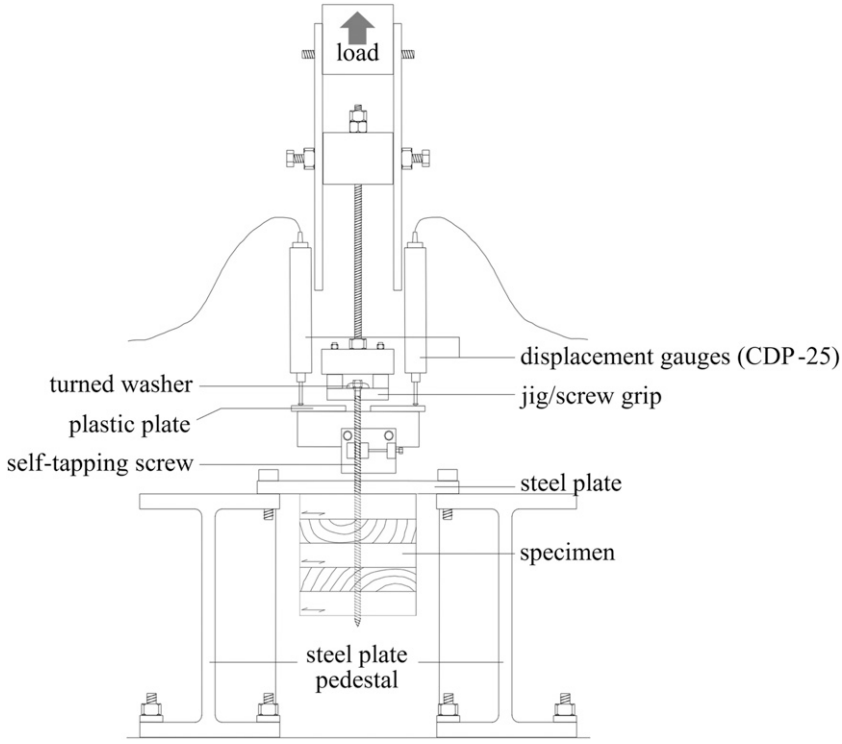

Figure 3. Test apparatus used to determine withdrawal capacity.

75% confidence level, which was 2.104 for ten replicates of each series, and *CV* denotes the coefficient of variation, obtained from the ratio of the standard deviation to the mean value.

The given characteristic withdrawal parameter in EN 1995-1-1:2004/A1 (2008) originated from the experiment by Blaß et al (2006), with the designed probabilistic model of withdrawal capacity for a single specimen and mean values derived in the following equation:

$$R_{\mathrm{ax},s(\mathrm{mean})} = 0.6 d^{0.5} l_{ef}^{0.9}\ \rho^{0.8}, \qquad (9)$$

This equation was divided by the divisor values in Eq 5 to predict the single specimen and mean values of withdrawal strength and then derived as follows:

$$f_{\mathrm{ax},s(\mathrm{mean})} = \frac{0.6 d^{-0.5} l_{ef}^{0.1}\ \rho^{0.8}}{\pi}, \qquad (10)$$

RESULTS AND DISCUSSION

Relationship between Withdrawal Load and Displacement

The different values of f_{ax} for each specimen series are shown in the boxplots in Fig 4, and the average values are listed in Table 2. The lowest average f_{ax} was obtained for the partially threaded STS on the jabon CLT-B specimen with a value of 3.4 N/mm^2, and the highest average value was obtained from the partially threaded STS on the karamatsu CLT-A specimen (9.15 N/mm^2). The f_{ax} values of the partially threaded STSs were higher than those of the fully threaded STSs for the CLT-A, CLT-C, and GLT specimens. However, the differences were not significant for the CLT-B specimens. Within a uniform thread diameter, when the withdrawal load is applied perpendicular to the grain, the shorter the l_{ef}, the higher the f_{ax}, which is a consequence of the divisor variable in Eq 5. Claus et al (2022)

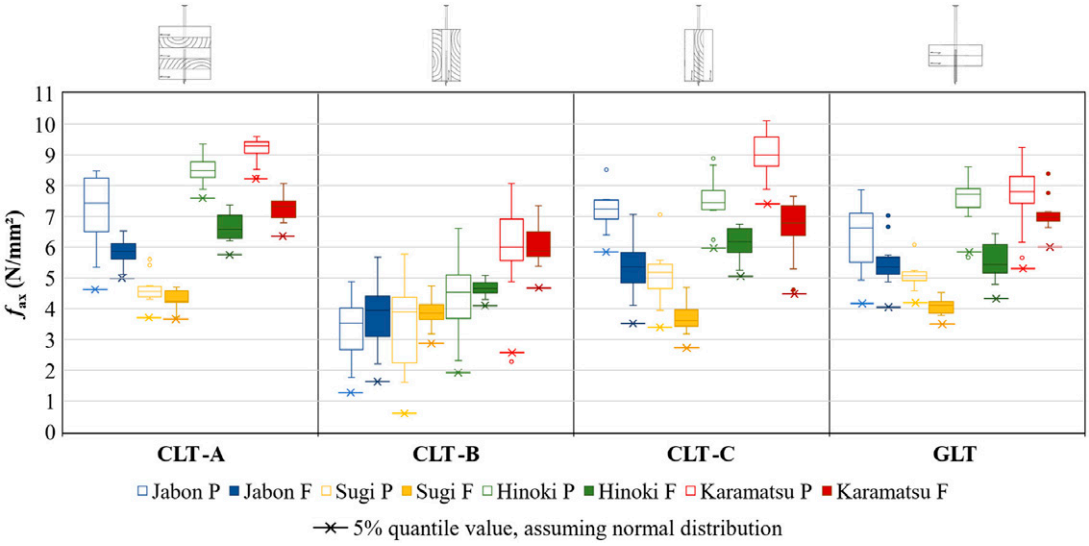

Figure 4. Boxplot of withdrawal strength for lamina species, the effective insertion length of STS-threaded part, and insertion points.

investigated force distribution along STSs using fiber Bragg grating measurements and found that force distribution on an STS insertion of length 270 mm into a GLT material was relatively constant when the screw axis to the grain angle was 0°. When the screw axis to the grain angle was 90°, the withdrawal force tended to be higher at the uppermost screw thread, which then gradually decreased to the lower end of the inserted screw thread. The results support previous literature that the length of the inserted threaded part of the STS did not significantly affect withdrawal force when it was inserted parallel to the grain.

Similar patterns were observed in the CLT-A, CLT-C, and GLT specimens when the angle between the STS axis and wood grain was 90°. However, the withdrawal load was applied in the radial direction of the wood in the CLT-A and GLT specimens, whereas in the CLT-C specimens, the withdrawal load was applied in the tangential direction of the adjacent wood, which in some way altered the failure mode, as discussed later.

Evaluation of the Prediction Model of Withdrawal Strength

The characteristic withdrawal strength of a single screw in EN 1995-1-1:2004/A1 (2008) is basically described by the characteristic density values for European softwood solid timber (EN 338 2016) and GLT (EN 1194 1999) provided in the Eurocode standards. For the materials used in this study, the individual specimen and the mean values of withdrawal strength were compared with the predicted value calculated by Eq 10, and 5%-quantile values of the experimental results to the predicted value calculated by Eq 7.

Significant correlations between the experimental results and predicted values by Eq 10 were found for GLT, CLT-A, and CLT-C when every single specimen within the series was analyzed, as shown in Fig 5. Significant correlations were noted when mean values were projected onto both the experimental results and predicted values obtained using Eq 10, as shown in Fig 6, for each specimen within the series. Figure 7 shows a comparison of the 5%-quantile values of the experimental results and those predicted using Eq 7. Significant correlations were observed for the GLT, CLT-A, and CLT-C specimens; however, the correlations were lower in CLT-B specimens. The decreased correlations for CLT-B specimens proved that the empirical model in EN 1995-1-1:2004/A1 (2008) was intended to determine the withdrawal capacity of joints with angles between

Table 2. The mean values of F_{ax} and f_{ax} for each series.

					F_{max}		f_{ax}	
Series	Species	Screw type	Specimen type	*n* #	Mean (kN)	CoV (%)	Mean (N/mm^2)	CoV (%)
S.P.GLT	Sugi	Partially threaded	GLT	10	4.09	8.15	5.09	8.15
S.P.CLT-A			CLT-A	10	9.44	9.69	4.70	9.69
S.P.CLT-B			CLT-B	10	7.04	38.83	3.50	38.83
S.P.CLT-C			CLT-C	10	10.42	16.11	5.18	16.11
S.F.GLT		Fully threaded	GLT	10	5.24	6.69	4.10	6.66
S.F.CLT-A			CLT-A	10	13.79	6.90	4.32	6.84
S.F.CLT-B			CLT-B	10	11.82	12.24	3.91	12.14
S.F.CLT-C			CLT-C	10	11.29	12.47	3.74	12.43
J.P.GLT	Jabon	Partially threaded	GLT	10	5.15	16.44	6.41	16.44
J.P.CLT-A			CLT-A	10	14.44	16.80	7.18	16.80
J.P.CLT-B			CLT-B	10	6.84	29.15	3.40	29.15
J.P.CLT-C			CLT-C	10	14.79	9.69	7.36	9.69
J.F.GLT		Fully threaded	GLT	10	6.94	12.84	5.58	12.82
J.F.CLT-A			CLT-A	10	18.20	6.91	5.85	6.83
J.F.CLT-B			CLT-B	10	11.35	27.29	3.82	26.73
J.F.CLT-C			CLT-C	10	16.39	16.01	5.37	16.10
H.P.GLT	Hinoki	Partially threaded	GLT	10	6.06	10.62	7.54	10.62
H.P.CLT-A			CLT-A	10	17.13	5.16	8.52	5.16
H.P.CLT-B			CLT-B	10	8.95	26.57	4.45	26.57
H.P.CLT-C			CLT-C	9	15.25	10.04	7.59	10.04
H.F.GLT		Fully threaded	GLT	10	7.13	10.59	5.59	10.56
H.F.CLT-A			CLT-A	10	21.23	6.01	6.67	6.45
H.F.CLT-B			CLT-B	10	14.15	5.80	4.68	5.64
H.F.CLT-C			CLT-C	10	18.37	8.22	6.15	8.34
K.P.GLT	Karamatsu	Partially threaded	GLT	10	6.19	14.69	7.70	14.69
K.P.CLT-A			CLT-A	10	18.39	4.82	9.15	4.82
K.P.CLT-B			CLT-B	10	11.90	26.58	5.92	26.58
K.P.CLT-C			CLT-C	10	18.07	8.18	8.99	8.18
K.F.GLT		Fully threaded	GLT	10	9.06	7.73	7.14	7.49
K.F.CLT-A			CLT-A	10	23.18	5.06	7.33	6.21
K.F.CLT-B			CLT-B	10	18.69	11.17	6.16	11.30
K.F.CLT-C			CLT-C	10	19.97	15.13	6.60	15.14

the STS axis and the grain direction (α) not less than 30°. Uibel and Blaß (2007) have proposed the corresponding prediction model for screw insertion parallel to the grain direction of European spruce (*Picea abies*) wood with the spacing requirements to prevent splitting. However, this proposed model was not qualified for a wide range of densities and was not included in the current regulation.

The relative corresponding linearities were shown for GLT specimens (Figs 5, 6, and 7) as the characteristic of GLT configurations considerably resembles solid wood, which was the intended purpose of the empirical model in EN 1995-1-1:2004/A1 (2008). The wide range of density distributions in the CLT layers modifies the withdrawal strength values predicted using Eq 7.

The single specimen, mean, and 5%-quantile values predicted using both empirical models in Blaß et al (2006) and EN 1995-1-1:2004/A1 (2008), except for CLT-B specimens, did not overestimate the experimental results, which was the expected for structural designing. Comparisons between values predicted using the empirical model in EN 1995-1-1:2004/A1 (2008) with the calculated experimental values indicated that the

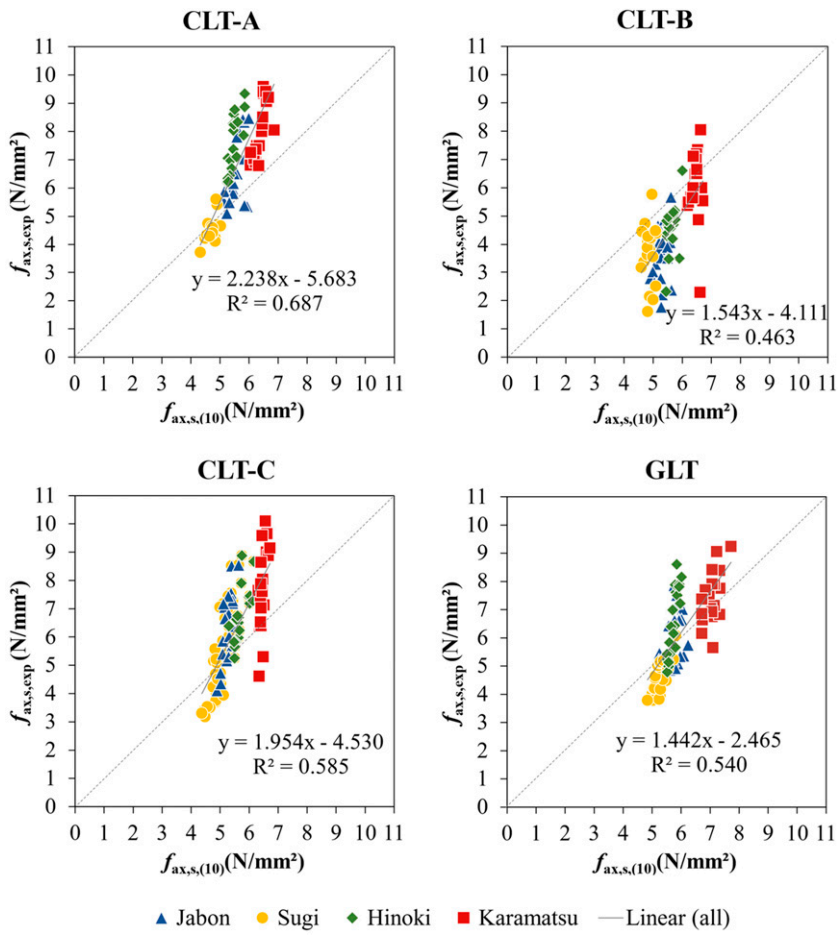

Figure 5. The comparison of individual experimental results and predicted values by Eq 10.

empirical model (Eq 7) was only suitable for the specimens with STSs insertion perpendicular to the grain direction (90°).

Even though the low withdrawal strength values of STSs inserted parallel to the grain (CLT-B) from experimental results implicitly remind us that the installation of STS in the narrow edge parallel to the grain should be avoided (Uibel and Blaß 2013), the author proposed the new probabilistic model approach for CLT-B specimens for the anticipatory step in any circumstances. The relationship between f_{ax} and density is usually described by a power regression model of the form $f_{ax} = a\rho^b\varepsilon$ where a and b are the regression parameters, with a as scaling and b as power parameter, and ε as the error/randomness in the regression model (Brandner 2019). According to Eq 7 in EN 1995-1-1:2004/A1 (2008), the effective insertion length of STS-threaded part, l_{ef} is also described by a power model. Therefore, the predicted withdrawal strength regarding wood density and the effective insertion length of STS were described by following formula, with a as scaling, b and c as power parameters.

$$f_{ax,\,pred} = a\rho^b l_{ef}{}^c \tag{11}$$

The substitution variables for the equation above were obtained to minimize the sum of quadratic differences between the whole experimental results and the proposed prediction model

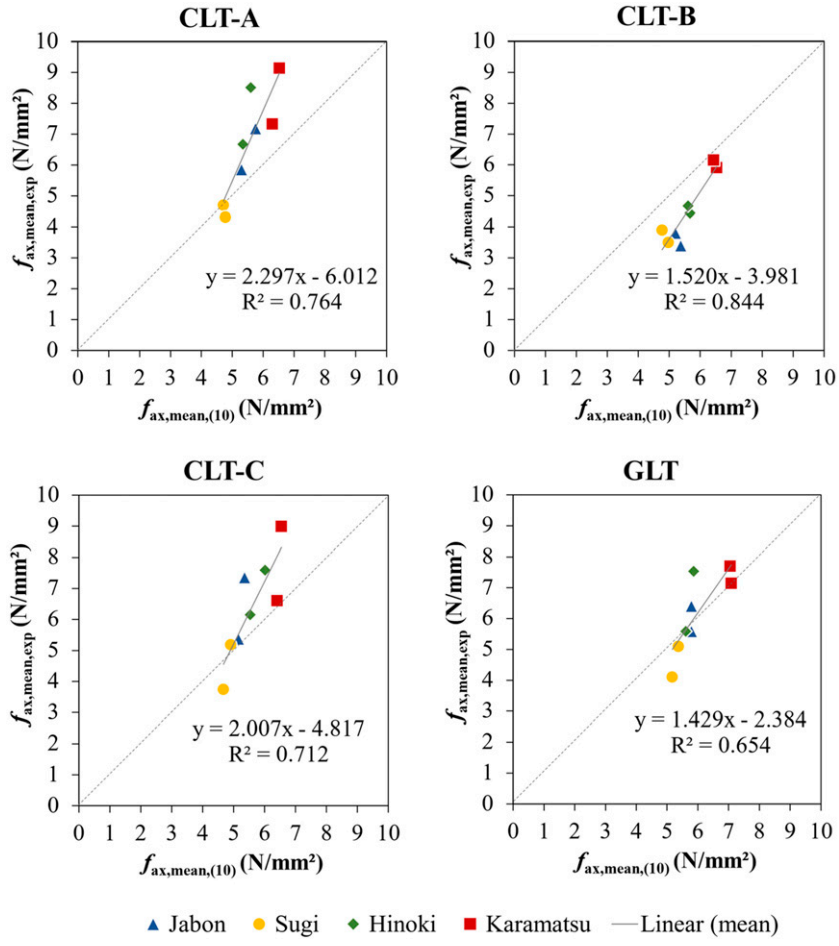

Figure 6. The comparison of mean experimental results and predicted values by Eq 10.

Therefore, the new prediction model for CLT-B specimens with the uniform STS thread diameter at 8 mm was derived as follows. This proposed model included the π division factor in the equation.

$$f_{ax,\,pred} = 0.000226 l_{ef}^{\,0.08} \rho^{1.6} \qquad (12)$$

The proposed prediction model for CLT-B was evaluated by linear regressive analysis with each specimen, mean, and 5%-quantile values of the experimental series results as projected in Fig 8(a)-(c), respectively. Linearity was obtained when the overall values of the experimental results and the predicted values calculated from the proposed Eq 12 were compared. The more significant linearity was found if the mean withdrawal strength of each series were compared. The 5%-quantile of predicted values from the proposed model in Eq 12 overestimated the 5%-quantile values of experimental results at the near-threshold significance level within the limited parameters in this study. There might be also other wood anatomical parameters which possibly have an influence on the withdrawal strength (Brandner 2019). Eq 12 was proposed for the withdrawal strength of STS insertion in the narrow side of CLT with parameters limited in this study; $d = 8$ mm, $\alpha = 0°$, the range of ρ 372-542 (kg/m^3), and the range of l_{ef} 80-120.8 mm. However, Eq 11 does not rule out the possibility for designing a more varied range of parameters.

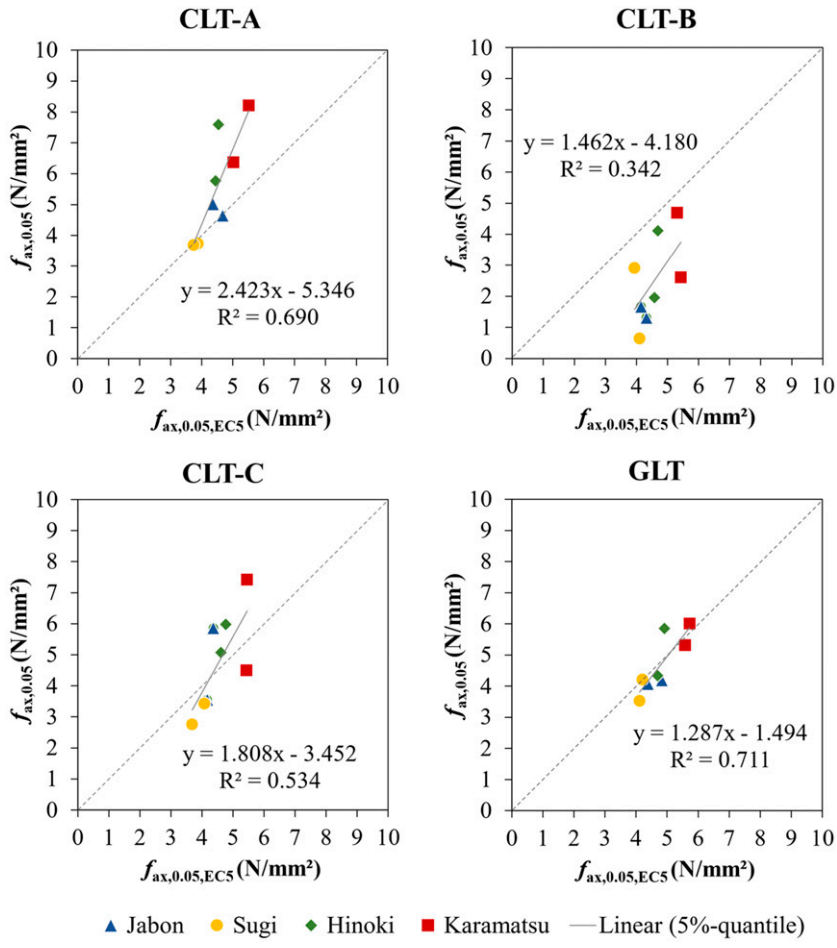

Figure 7. The comparison of 5%-quantile experimental results and predicted values by Eq 7.

The experimental values were further evaluated with the recently given probabilistic model in response to the overestimated 5%-quantile values predicted with Eq 12. Ringhofer et al (2018) proposed a generic approach which covered the thread-grain angle α $\{0, 90\}^\circ$ generated from experimental data of solid softwood C24 with characteristic density of 350 (kg/m^3) according to EN 338 (2016), derived as the simplified following equations:

$$f_{ax,k,R} = k_{ax,k}\ k_{sys,k}\ 8.67 d^{-0.33} \left(\frac{\rho_k}{350}\right)^{k_\rho}, \quad (13)$$

$$k_{ax,k} = \begin{cases} 1.00 & \text{for } 45^\circ \le \alpha \le 90^\circ \\ 0.58 + 0.0094\alpha & \text{for } 0^\circ \le \alpha \le 45^\circ, \end{cases} \quad (14)$$

$$k_{sys,k} = 1.00 \quad \text{for solid timber and CLT, } N \ge 3, \quad (15)$$

$$k_\rho = \begin{cases} 1.10 & \text{for } 0^\circ < \alpha \le 90^\circ, \\ 1.25 - 0.05d & \text{for } \alpha = 0^\circ \end{cases} \quad (16)$$

However, the probabilistic model in Eqs 13-16 did not effectively predict the withdrawal strength of 5%-quantile values of CLT-B specimens with the coefficient of determination R^2 0.499. The limited characteristic density for designing an equation restricted the range of applicable parameters. Besides, the input parameters in this study also need to be evaluated.

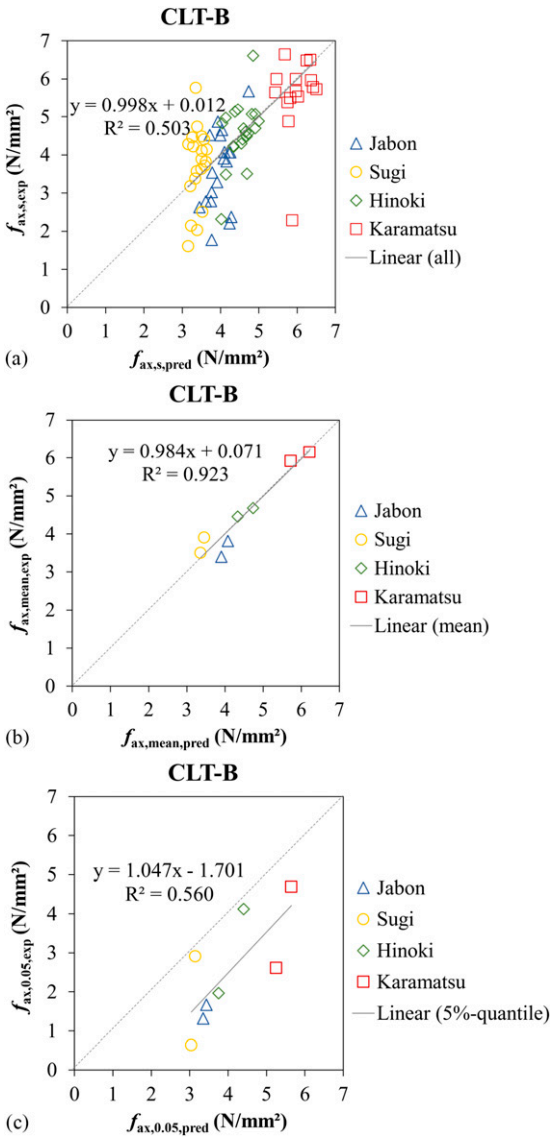

Figure 8. Correlation between the experimental results and the proposed predicted values by Eq 12: (a) individual specimens; (b) mean; (c) 5%-quantile.

The projected ρ values to Eqs 7, 10, and 12 generated a disproportionate distribution on withdrawal strength when the STS insertion point was on the narrow side, CLT-B and CLT-C. This is possibly the causative effect of the unspecific value of ρ which is the mean value of the density of the whole laminas used for CLT layers instead of the STS-adjacent CLT layer density. The range of densities measured from the specimens in this study was also considered too large to be predicted using Eq 7, where this empirical model was derived for European softwood (EN 338 2016).

Influence of Parameters to Withdrawal Strength

Density, ρ, was the only wood characteristic which considerably influenced withdrawal strength in this study, and the effective insertion length of the STS-threaded part, l_{ef}, was the representative geometrical aspect of STS. Within the limited range of the above parameters, the significant influences on the withdrawal strength of STS analyzed through linear regression indicated by the coefficient of determination, R^2. As shown in Fig 9, lamina density within species significantly influenced withdrawal strength as indicated by the regression equations found on S.F.CLT-A, S.F.CLT-C, H.F.GLT, H.F.CLT-A, H.F.CLT-B, K.F.CLT-A, S.P.GLT, and S.P.CLT-A. Jabon specimen density had no significant effect on withdrawal strength. Brandner (2019) found that the withdrawal strength of screws inserted in hardwood increased disharmonious with increasing density, but that was not the case in softwood (Uibel and Blaß 2007).

The effective insertion length of the STS-threaded part had significant negative effects on the withdrawal strength of sugi and hinoki GLT, hinoki and karamatsu CLT-A, and a whole specimen of CLT-C (Fig 10). This negative effect of l_{ef} was also reasonably interpreted by the power value in the empirical model, Eq 6. None of wood species in CLT-B specimens were significantly influenced by the l_{ef} parameter, which is in line with the excluded l_{ef} parameter in the generalized-angle ($0° \leq \alpha \leq 90°$) proposed empirical model in previous studies (Ringhofer et al 2018; Brandner 2019) where no further length effect was considered in the calculation, as the l_{ef} did not cover the tip length.

Failure Modes

The angle between the STS axis as well as the withdrawal load direction and the grain direction,

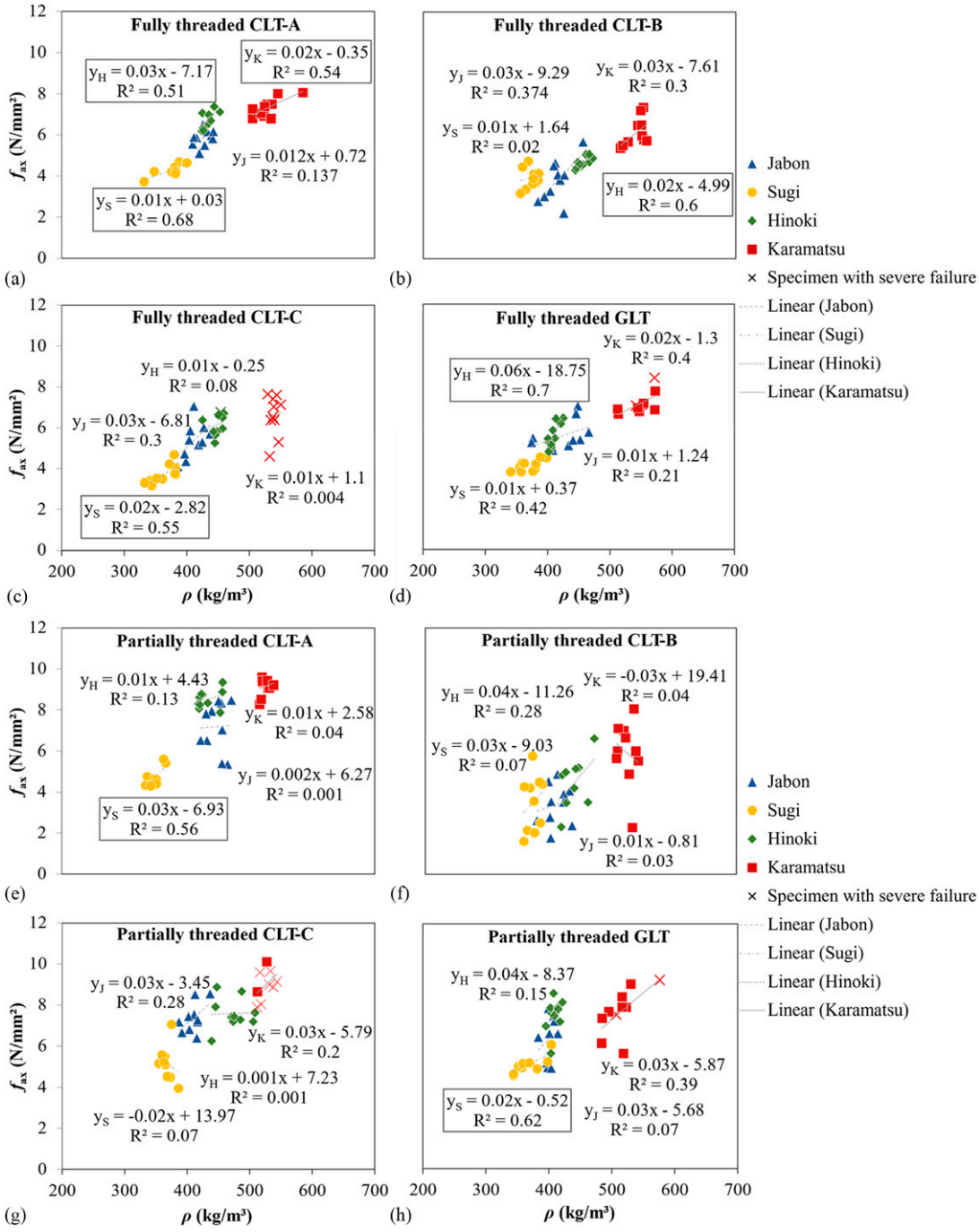

Figure 9. The linear regression analyses of withdrawal strength vs lamina density: (a)-(d) specimens with fully threaded STS and (e)-(h) specimens with partially threaded STS.

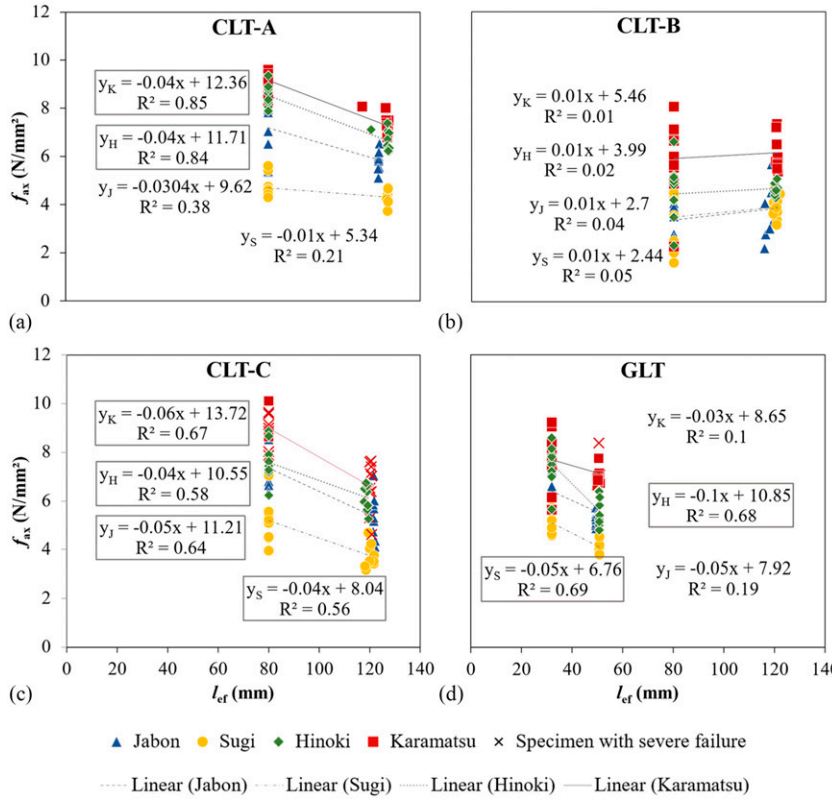

Figure 10. Linear regression analyses of withdrawal strength vs effective insertion length of the STS-threaded part.

was grouped as either 0° or 90°. The CLT-B specimen was the only specimen configuration which is inserted with the STS parallel to the grain (0°). The CLT-A, CLT-C, and GLT were technically inserted with the STS perpendicular to the grain (90°). However, a difference was observed on the orthotropic anatomy of the wood materials. The STS was inserted in the radial direction through the crossed layup configuration in the CLT-A specimen. The STS insertion in the unidirectional layups was subjected to the GLT model in the same direction as CLT-A. And the direction of STS insertion to the CLT-C was in tangential. According to the mentioned conditions, the typical forms of failure modes were observed.

In this study, the failure modes were divided into three categories. First, the withdrawal failure, which is an initial failure in withdrawal test, characterized by the shear failure at the wooden members surrounding the STS which was sticking out of the upmost layer of CLT around the STS (Pang et al 2020), depicted in Fig 11. The second failure mode was a crack perpendicular to the withdrawal test direction (Fig 12) and the third

Figure 11. Typical withdrawal failure mode showing pull out of uppermost layer on specimen K.F.CLT-A_2.

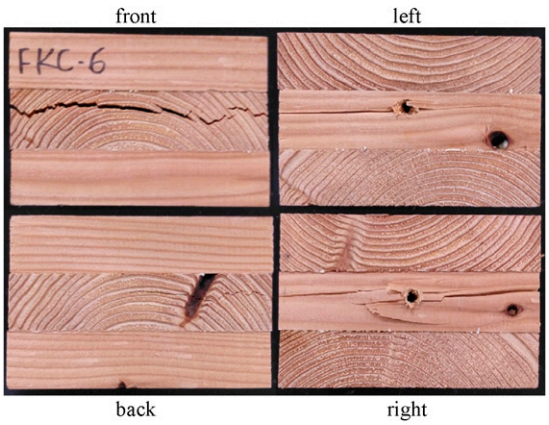

Figure 12. Typical crack failure mode on specimen K.F.CLT-C_6.

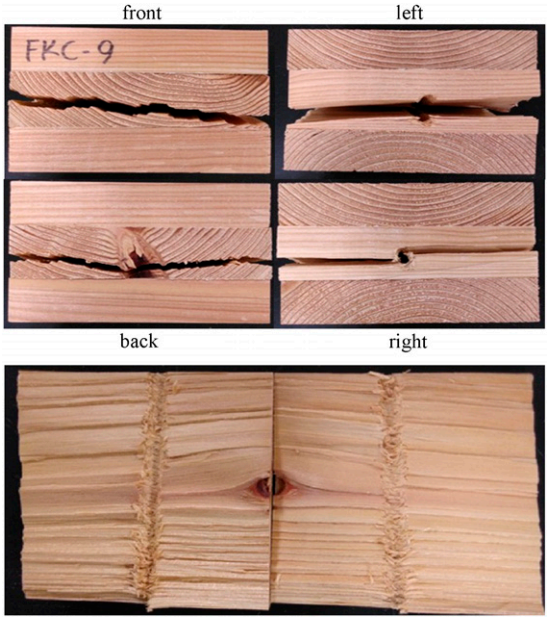

Figure 13. Typical split failure mode on specimen K.F.CLT-C_9.

failure mode was split as the further impact of the crack represented in Fig 13 were categorized into severe damage.

Withdrawal failure modes were found in all specimens before the damage continued to increase. Crack failures occurred on one specimen of H.F.CLT-C, six K.F.CLT-C, seven K.P.CLT-C, one K.F.GLT, and two K.P.GLT. Four K.F.CLT-C, one K.P.CLT-C, and one K.F.GLT were found with split failures. The severe failures with cracks and splits mostly occurred on the dense specimens in tangential to the withdrawal force. Similar failures were observed by Xu et al (2021) who noted splitting and tension cracks perpendicular to the grain in the first layer of CLT karamatsu. Severe failures were also found on some dense GLT specimens. This would be the important case for the spacing method of STS on the narrow edge of dense wood material in the tangential direction and in dense unidirectional layups or solid wood in the radial direction. These results also suggest that the cross-lamination method might help prevent severe failures. The spacing protocols for STS installation on the narrow edge of CLT are available as suggested in Uibel and Blaß (2007) and ETA-11/0030 (2019) to ensure a reliable design.

CONCLUSIONS

The properties of fast-growing jabon were investigated to determine its potential for structural purposes, compared with common commercial Japanese softwoods listed in JAS 3079-2013. Withdrawal strength (f_{ax}) was determined for a state-of-art STS and timber material; CLT and GLT were investigated within the bandwidth of parameters of density (ρ), the effective insertion length of the threaded part of the STS (l_{ef}), and the side of CLT where the screw was installed. EN 1995-1-1:2004/A1 (2008) has been used in Japan and was evaluated for 5%-quantile characteristic values along with the basic empirical approach given in Eq 10 for the single specimen values and mean values. With a uniform thread diameter (d) 8 mm, the influences of ρ and l_{ef} were investigated.

- A preliminary test was carried out on the lamina material to determine the bending Young's modulus E_b passed the minimum grade according to the lamina classification in JAS 3079-2013 before considering its structural potential for jabon as fast-growing species.

- Within the density (ρ) and the effective insertion length of threaded part of STS (l_{ef}) bandwidth in this study, the withdrawal strength of fully threaded and partially threaded STS inserted into the different sides of CLT as well as GLT made of jabon, sugi, hinoki, and karamatsu lamina was evaluated. The result showed that the withdrawal strength of the partially threaded STS was higher than fully threaded STS when it was inserted perpendicular to the grain, yet was not the pattern in the STS inserted parallel to the grain of the specimen, regarding the difference in stress distribution along the STS. However, it should be highlighted that the withdrawal strength of the STS is relative to the l_{ef} as the divisor variable in the formulation.
- The compatibility of the probabilistic model given in EN 1995-1-1:2004/A1 (2008) (Eq 7) on predicting the 5%-quantile value of withdrawal strength and the given probabilistic model in Blaß et al (2006) (Eq 10) on predicting the single specimen and mean values with the limited parameters bandwidth in this study have been evaluated. It was found that the probabilistic model is beneficial in predicting the withdrawal strength of the STS when the predicted values underestimated the experimental results concerning the purpose of the empirical model is to predict the worse possibility yet correspond to the experiment result. Both equations unlikely effective in predicting a withdrawal strength for STS insertion parallel to the grain in the narrow side of CLT (CLT-B), proving the regulation projected for the angle between the STS axis and the grain direction (α) is not less than 30°.
- A new empirical approach was proposed for CLT-B in Eq 12. The proposed model was particularly effective in predicting the withdrawal strength of single specimen, mean, and 5%-quantile values of the experiment. However, the overestimation of 5%-quantile values still requires a further solution.
- The significant influence of the lamina density was not found in every wood species and the insertion point of the STS due to the unspecific measurement of density on the STS-inserted wood member. The effective insertion length of the STS-threaded part seemed to influence the withdrawal strength if it was inserted in the tangential direction of the wood member.
- According to the observed failure modes, the spacing design of STS installment on the narrow side perpendicular to the grain and plane side of dense wood member need to be concerned to prevent severe failure caused by withdrawal force.

ACKNOWLEDGMENTS

The brief results of this experiment were presented in an online poster presentation at the 71st Japan Wood Society Conference in March 2021.

In preparation for the experiment, the authors were assisted by Tomoki Shinohara, a second year Master student in the fiscal year 2020. Our gratitude goes to him.

CONFLICT OF INTEREST

The authors declare that they have no potential conflict of interest that could have influenced the works reported in this paper.

REFERENCES

AIJ (Architectural Institute of Japan) (2006) Standard for structural design of timber structure (in Japanese). Architectural Institute of Japan, Tokyo. 153 pp.

Blaß H, Bejtka I, Uibel T (2006) Load-bearing capacity of connections with fully threaded self-drilling wood screws. University of Karlsruhe (TH), Chair of Timber Engineering and Structural Design. Karlsruhe University Press, Karlsruhe, Germany (in Germany).

Brandner R, Ringhofer A, Grabner M (2018) Probabilistic models for the withdrawal behavior of single self-tapping screws in the narrow face of cross laminated timber (CLT). Eur J Wood Prod 76(1):13-30.

Brandner R (2019) Properties of axially loaded self-tapping screws with focus on application in hardwood. Wood Mater Sci Eng 14(5):254-268. https://doi.org/10.1080/17480272.2019.1635204.

Claus T, Seim W, Küllmer J (2022) Force distribution in self-tapping screws: Experimental investigations with

fibre Bragg grating measurement screws. Eur J Wood Prod 80(1):183-197.

Dietsch P, Brandner R (2015) Self-tapping screws and threaded rods as reinforcement for structural timber elements - A state-of-the-art report. Constr Build Mater 97:78-89. https://doi.org/10.1016/j.conbuildmat.2015.04.028.

EN 1382 (1999) Timber structures – Test methods: Withdrawal capacity of timber fasteners. European Committee for Standardization (CEN), Brussels, Belgium.

EN 1995-1-1 (2004) Eurocode 5: Design of timber structures – Part 1-1: General – Common rules and rules for buildings. European Committee for Standardization (CEN), Brussels, Belgium. Pages 77-78.

EN 1995-1-1:2004/A1 (2008) Eurocode 5: Design of timber structures - Part 1-1: General - Common rules and rules for buildings. European Committee for Standardization (CEN), Brussels, Belgium. Pages 12-13.

EN 338 (2016) Structural timber - Strength classes. European Committee for Standardization (CEN), Brussels, Belgium. p. 7.

EN 1194 (1999) Timber structures—Glued laminated timber. Strength classes and determination of characteristic values. European Committee for Standardization (CEN), Brussels, Belgium. 7 pp.

ETA-11/0030 (2019) European Technical Assessment ETA-11/0030: Rotho Blaas self-tapping screws and threaded rods. European Organisation for Technical Assessment – EOTA, Brussels, Belgium. Pages 8-9.

Goto Y, Jockwer R, Kobayashi K, Karube Y, Fukuyama H (2018) Legislative background and building culture for the design of timber structures in Europe and Japan. Pages 8-9 *in* WCTE 2018, World Conference on Timber Engineering, Seoul, Republic of Korea.

Izzi M, Casagrande D, Bezzi S, Pasca D, Follesa M, Tomasi R (2018) Seismic behaviour of Cross-Laminated Timber structures: A state-of-the-art review. Eng Struct 170:42-52.

JIS Z 2101 (2009) Methods of test for woods. Japanese Industrial Standard.

Kobayashi K (2015) Present and future tasks for screw joints in timber structures. Mokuzai Gakkaishi 61(3): 162-168 (in Japanese).

Krisnawati H, Kallio M, Kanninen M (2011) Anthocephalus cadamba Miq.: Ekologi, Silvikultur dan Produktivitas [Anthocephalus cadamba Miq.: Ecology, Silviculture dan Produktivity]. Center for International Forestry Research, Bogor.

Mahdavifar V, Sinha A, Barbosa AR, Muszynski L, Gupta R (2018) Lateral and withdrawal capacity of fasteners on hybrid cross-laminated timber panels. J Mater Civ Eng 30(9):1-11. 04018226.

Mansur I, Tuheteru FD (2010) Kayu Jabon [Jabon Wood]. Penebar Swadaya, Jakarta (in Indonesian).

Mohammad M, Douglas B, Rammer D, Pryor SE (2013) Chapter 5 - Connections in cross-laminated timber buildings. Pages 3-44 *in* E Karacabeyli and B Douglas, eds. CLT handbook: Cross-laminated timber. FPInnovations, Canada.

Okuda S, Corpataux L, Muthukrishnan S, Wei KH (2018) Cross-laminated timber with renewable, fast-growing tropical species in Southeast Asia. Pages 1-2. *in* World Conference on Timber Engineering, 2018, WCTE, Seoul, Republic of Korea.

Pang SJ, Ahn KS, Kang SG, Oh JK (2020) Prediction of withdrawal resistance for a screw in hybrid cross-laminated timber. J Wood Sci 66(1):1-11.

Passarelli RN, Koshihara M (2018) The implementation of Japanese CLT: Current situation and future tasks. *in* World Conference on Timber Engineering. 2018, WCTE, Seoul, Republic of Korea.

Ringhofer A, Brandner R, Schickhofer G (2015) Withdrawal resistance of self-tapping screws in unidirectional and orthogonal layered timber products. Mater Struct 48(5):1435-1447. doi:10.1617/s11527-013-0244-9.

Ringhofer A, Brandner R, Blaß HJ (2018) Cross laminated timber (CLT): Design approaches for dowel-type fasteners and connections. Eng Struct 171:849-861.

Uibel T, Blaß HJ (2007) Edge joints with dowel type fasteners in cross laminated timber. Pages 6-11 *in* Proceedings, International Council for Research and Innovation in Building and Construction Working Commission W18 - Timber Structures (CIB-W18/40-7-2), Bled, Slovenia.

Uibel T, Blaß HJ (2013) Joints with dowel type fasteners in CLT structures. Pages 119-134 *in* European Conference on Cross Laminated Timber, Graz, Austria.

Xu J, Zhang S, Wu G, Gong Y, Ren H (2021) Withdrawal properties of self-tapping screws in Japanese larch (*Larix kaempferi* (Lamb.) Carr.) cross laminated timber. Forests 12(5):524-13.